A Numerical and Asymptotic Study of Some Third-Order Ordinary Differential Equations Relevant to Draining and Coating Flows

E. O. Tuck, L. W. Schwartz

SIAM Review, Volume 32, Issue 3 (Sep., 1990), 453-469.

SIAM REVIEW
Vol. 32, No. 3, pp. 453–469, September 1990

003

A NUMERICAL AND ASYMPTOTIC STUDY OF SOME THIRD-ORDER ORDINARY DIFFERENTIAL EQUATIONS RELEVANT TO DRAINING AND COATING FLOWS*

E. O. TUCK†‡ AND L. W. SCHWARTZ†

Abstract. Some draining or coating fluid-flow problems, in which surface tension forces are important, can be described by third-order ordinary differential equations. Accurate computations are provided here for examples such as $y'''(x) = -1 + 1/y^2$ that permit the boundary condition $y \to 1$ as $x \to -\infty$, so modelling a layer of fluid that is asymptotically uniform behind the draining front. The ultimate fate of the solution as x increases is studied for the above example, and for a generalisation involving a small parameter δ such that this example is recovered in the limit as $\delta \to 0$, but which is such that $y \to \delta$ as $x \to +\infty$, so modelling draining over an already-wet surface. Matched asymptotic expansions are then used to derive limiting results for small δ, this being a singular perturbation since the problem with $\delta = 0$ does not permit $y = 0$. The physical basis for this singularity is the well-known impossibility of moving a contact line over a dry nonslip surface. Other modifications that avoid the singularity by allowing slip are also discussed.

Key words. differential equations, nonlinear, fluid dynamics, draining

AMS(MOS) subject classifications. 34B15, 34E05, 76O99

1. Introduction. Fluid dynamic problems involving surface tension forces are described in general by partial differential equations in space and time, with rather high, typically fourth-order, spatial differentiations. For example, the thickness y of a thin film of viscous fluid draining over a solid surface in an unsteady manner satisfies such an equation. In some cases, as for example at the front edge of a large drop of fluid moving on a plane surface, the flow can be treated as steady in a frame of reference moving with the front. If, in addition, there is only one spatial coordinate of interest, namely, that in the direction of motion along the plane, the problem has reduced to an ordinary differential equation in that variable, say x. Further, the original fourth-order system then permits one explicit integration, effectively due to conservation of mass, and the result is an autonomous third-order ordinary differential equation of the form

$$\frac{d^3y}{dx^3} = f(y)$$

for some given function $f(y)$.

The actual form of this function $f(y)$ varies according to the physical context, and we consider here some simple rational-function forms, namely,

$$f(y) = -1 + y^{-2}, \tag{1.1}$$

$$f(y) = -1 + (1 + \delta + \delta^2)y^{-2} - (\delta + \delta^2)y^{-3}, \tag{1.2}$$

$$f(y) = y^{-2} - y^{-3}, \tag{1.3}$$

$$f(y) = y^{-2}, \tag{1.4}$$

*Received by the editors April 26, 1989; accepted for publication (in revised form) January 19, 1990.

†Department of Mechanical Engineering, University of Delaware, Newark, Delaware 19716.

‡Permanent address, Applied Mathematics Department, University of Adelaide, S.A. 5001, Australia.

$$f(y) = -1 + (1+\alpha)/(y^2+\alpha), \tag{1.5}$$

$$f(y) = -1 + (1+\alpha)/(y^2+\alpha y). \tag{1.6}$$

Equation (1.1) is of the greatest interest, and is relevant to fluid draining problems on a dry wall, involving the forces of viscosity, gravity and surface tension, subject to a lubrication approximation. However, its solution has some unacceptable features when y is small, associated ultimately with the impossibility of moving a contact line $y = 0$ over a nonslip truly dry wall. Equation (1.2) is a generalisation to a coating problem, or to draining over a wet wall, that sidesteps these difficulties when δ is a small positive parameter measuring wall wetness. Careful numerical solutions of both (1.1) and (1.2) are provided here, and in particular we find 4-figure accurate solutions of (1.2) subject to the boundary conditions that $y \to 1$ as $x \to -\infty$ and $y \to \delta$ as $x \to +\infty$.

Equation (1.1) is a model for some more complicated problems whose description may involve partial differential equations in more than one space dimension and time, or may involve more physical and geometrical complexity. In such cases, the generalisation (1.2), while in principle avoiding the small-y paradox suffered by (1.1), may be computationally infeasible, or at least "stiff" in the sense that the relevant value of δ may be very much smaller than the computational grid size. This numerical difficulty is also common to other generalisations of (1.1) discussed below, such as (1.5) or (1.6), which also reduce to (1.1) when $\alpha = 0$.

Hence there is a powerful incentive to use (1.1) as it stands, which can be justified and aided by an asymptotic study of the formal limit of solutions of (1.2) as $\delta \to 0$. This is provided here by matched asymptotic expansions, the solution of (1) being now viewed as an outer expansion with a singularity at $y = 0$.

Now we also need solutions of both (1.3) and (1.4). Equation (1.3) describes the inner expansion near the singularity, while equation (1.4) provides the link between the inner and outer expansions, being both the small-y limit of (1.1) and the large-y limit of (1.3).

It is an important and unusual feature of this class of asymptotic problem that the limiting solutions of (1.1) depend significantly on δ even when δ is (apparently absurdly) small. It is not enough to observe that so long as δ is nonzero, no paradox occurs; the actual value of δ matters.

The final result is a relationship connecting the maximum slope $\beta = \max|dy/dx|$ with the parameter δ, and this relationship can be interpreted in terms of an apparent contact angle for draining over a dry wall. That is, suppose that we cease computation of (1.1) at some extremely small (but not actually zero) value of y, at which point we demand that the downslope β be prescribed. The solutions of (1.1) then depend essentially on the value of β, while not depending significantly on the small value of y at which the computation is stopped. The parameter β may be determined as here by its relationship to a physically specified small parameter like δ, or may itself be viewed as empirical data. It plays the role of the tangent of a "contact angle," although it is not a unique physical property like the usual static contact angle, and in particular, actual contact does not occur.

The final section of the present paper discusses in considerably less detail equations (1.5) and (1.6), which arise via two different models common in the literature that allow "slip" of the fluid at the wall, and which both reduce to (1.1) when $\alpha \to 0$. By using either model, a contact point $y = 0$ is permitted for a range of (small positive) values of the slip parameter α. In the model (1.5), $y = 0$ is no longer a singular point, whereas for (1.6) the weakened singularity permits contact at either a zero or

finite angle. The results with slip are compared with those for the wetting-layer model (1.2), and some observations are made regarding relations between static and dynamic contact angles.

The present work is intended as a detailed and complete study of a simple well-defined mathematically-posed problem. The above differential equations are not new, all of them having been discussed to varying levels in complex applied contexts where the problem formulation was (inevitably) often ill defined, and where controversy was common. The remainder of this Introduction is a very brief literature survey, confined in the main to those studies that use a lubrication approximation. More comprehensive surveys are given by Dussan V. (1979), Ruschak (1985), de Gennes (1985), and Friedmann (1988).

Equation (1.3) is perhaps the most famous of the above equations, having been introduced by Landau and Levich (1942) (see Levich (1962, p. 680)) for a coating application, and used since in many studies of capillarity-dominated coating and other thin-film applications where gravity is negligible, e.g., by Bretherton (1961), Friz (1965), Spiers, Subbaraman and Wilkinson (1974), Tanner (1979), Wilson (1982), Schwartz, Princen and Kiss (1986). Equation (1.2) may be considered as a generalisation of (3) to include gravity in the coating problem; it is given explicitly by Levich (1962, p. 678), and is a special case of equations given by Atherton and Homsy (1976) and by Tuck and Vanden-Broeck (1984).

The genesis of equations such as (1.1) is more complicated, since there are many possible escapes from the paradox that arises when (1.1) is used blindly near $y = 0$, and thus (1.1) itself is not normally written down. Several authors (e.g., Greenspan (1978), Hocking (1981)) use equations equivalent to (1.5) or (1.6) that allow the fluid to slip near the contact point. Dussan (1976) solves the low Reynolds number equations for flow in a corner where the wall slip is prescribed. Others (see de Gennes (1985)) allow extra terms modelling short-range molecular (e.g., Van der Waals) forces. Both types of extra term are contained in a more general equation given in the appendix of Huh and Scriven (1971).

As indicated above, (1.1) has generalisations to globally more complicated problems, but in which the local difficulties at $y = 0$ are still present, e.g., Greenspan (1978), Greenspan and McCay (1981), Huppert (1982), Tuck, Bentwich, and Van Der Hoek (1983), Young and Davis (1987), Schwartz and Michaelides (1988), and Schwartz (1989). In some of these contexts, solutions have been presented in the limit as the surface tension tends to zero, a simplification which has its own paradoxes. In seeking to put surface tension back into these problems, we meet (1.1) or something similar; indeed Huppert (1982) would have derived (1.1) itself, were it not for an incorrect surface-tension term. There are singular perturbation problems (Howes (1983)) of a boundary-layer type quite different to the present one, associated with this limit of small surface tension.

The singular perturbation or matched approximation character of the near-contact problem is discussed with slip but without gravity by Cox (1986), and some model singular perturbation problems have been discussed by Young and Davis (1985). Tanner's (1979) study is perhaps the closest in spirit to the present paper, and he also matches solutions of (1.3) and (1.4) together, but does not include gravity. This work of Tanner has been used by de Gennes (1985) as a basis for a theory of apparent contact angle, a concept that has also been discussed by Hocking (1981).

2. Dry wall draining. Consider first the differential equation

$$\frac{d^3y}{dx^3} = -1 + y^{-2}. \tag{2.1}$$

This equation describes the thickness $y(x)$ of a layer of fluid that is draining down a vertical wall, the third-derivative term representing surface tension effects, the constant term on the right representing gravity, and the term in y^{-2} the viscous shearing forces. The special draining flow of interest is assumed steady in a frame of reference that is falling with the layer; hence there is an apparent upward movement of the wall in this frame. For example, we may hope to use the model to describe a situation like that of Fig. 1, where a semi-infinite mass of fluid is falling down an otherwise dry wall.

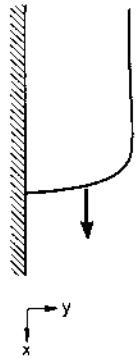

FIG. 1. *Sketch of idealised draining flow.*

Equation (2.1) clearly possesses the solution $y \equiv 1$. This is a uniform draining layer, and in the context of Fig. 1 may be thought of as the limiting configuration far above the leading edge of the layer. Thus we use a boundary condition of the form

$$y \to 1 \quad \text{as} \quad x \to -\infty. \tag{2.2}$$

A formal linearisation of (2.1) for small departures from this uniform state shows that (5.2) can be strengthened to

$$y \to 1 + a \exp\left[2^{-2/3}x\right] \cos\left[3^{1/2}2^{-2/3}x\right] \tag{2.3}$$

where a is a constant.

In fact, (2.3) specifies just one of the three linearly independent solutions of the linearised equation; one other is unbounded as $x \to -\infty$, and a third solution involving a sine instead of a cosine can be absorbed into an arbitrary choice of the origin of x. Hence we can expect to generate all solutions of (2.1) that satisfy (2.2) by specifying the input parameter a. Any algorithm for solving (2.1) subject to (2.3) will generate a one-parameter family of solutions, all satisfying (2.2).

However, the parameter a can be restricted to a finite interval of real positive values, since if $a = a_0$ generates the solution $y = y_0(x; a_0)$, then

$$y = y_0\left(x - \frac{2\pi}{3^{1/2}2^{-2/3}}; a_0 \exp\left[\frac{2\pi}{3^{1/2}}\right]\right) \tag{2.4}$$

is also a solution. Thus, multiplication of a by the factor $\exp[2\pi/\sqrt{3}] \approx 37.6224$ yields the identical solution, but simply shifted in x. A similar consideration shows that no

extra generality ensues from negative a. For definiteness, we allow a to lie in the range from about 0.001 to 0.038.

Numerical solution of (2.1) subject to (2.3) is straightforward. If we choose any starting point $x = x_0$, then we could simply call upon any convenient initial-value algorithm, with initial conditions on y, y', y'' given by assuming that (2.3) is accurate at that $x = x_0$. This will be true at any a if x_0 is sufficiently large and negative; equivalently, it is true at any x_0 if a is sufficiently small. Adopting the latter viewpoint, we may even take $x_0 = 0$. But now the accuracy of our results is dependent upon smallness of a, and even in the range of small a quoted above, there is a considerable benefit to be gained from inclusion in (2.3) of second-order corrections, i.e., terms of order a^2, and this was done routinely. We can check this truncation-error aspect of the accuracy of the computation by comparing computations at a given a value with those at $a/37.6224$, and (with the second-order corrections implemented) this comparison indicated that all results were accurate to better than four significant figures in the above a-range.

The actual method used was fourth-order Runge–Kutta, with a stepsize that was allowed to reduce with (in proportion to) y, when y is small and the solution is changing rapidly. Ample accuracy (i.e., with errors less than the above fourth-figure truncation error) was achieved by starting the computation with a stepsize of 0.05.

The (perhaps surprising) results are as follows. Solutions of (2.1) satisfying (2.2) neither take the value $y = 0$ nor approach $y = 0$ at any x. Every solution takes positive values as small or as large as we please, since every solution possesses an infinite number of maxima and minima, the minima taking positive values that become smaller and smaller in magnitude as $x \to +\infty$, while the maxima take values that become larger and larger as $x \to +\infty$.

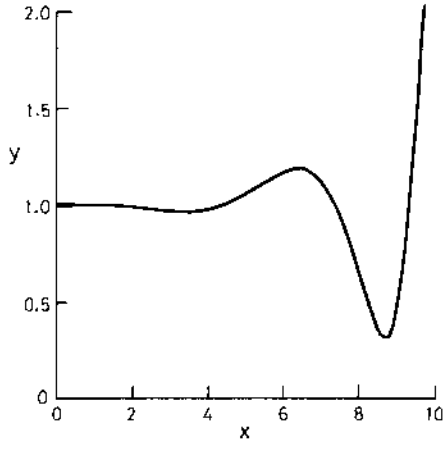

FIG. 2. *Example solution $y = y(x)$ for dry-wall draining at $a = 0.004$.*

Figure 2 shows a typical result, at $a = 0.004$. This graph indicates a "secondary" maximum of $y = 1.0047$ at $x = 0.48$, a "secondary" minimum of $y = 0.9716$ at $x = 3.33$, a "primary" maximum of $y = 1.1902$ at $x = 6.33$, then a "primary" minimum of $y = 0.3077$ at $x = 8.68$, after which y increases off the scale of the graph. But not forever; there follows a "super" maximum of $y = 160.81$ at $x = 21.23$, and a "super" minimum at $x = 27.46$, then we expect another even higher "super" maximum, etc. All the above quoted results are accurate to the quoted four figures for

the y-values; the actual value of the first "super" minimum is too small to compute, but is certainly less than 10^{-15}. The above classification in terms of " secondary," "primary," and "super" turning points reflects interest in realistic values of y; in particular, the "super" turning points are clearly nonphysical.

As the parameter a varies, there is a smooth interchange of the roles of the various maxima and minima. Thus if we increase a above 0.004, the "primary" minimum of $y = 0.3077$ steadily decreases in size until it looks more like a "super" minimum. For example, it reaches the (still four-figure accurate) value $y = 0.00000008692$ at $a = 0.025$. (It is this smooth transformation that inspires confidence that the "super" minima are not actually zero, even when too small to compute.) Meanwhile, the "secondary" minimum is also decreasing in size, and reaches (exactly!) the old primary value $y = 0.3077$ at $a = 0.004$ times $37.6224 = 0.150490$, etc. The real range of interest is one where there are "sensible" primary maxima and minima, namely, about $a = 0.0025$ to $a = 0.02$.

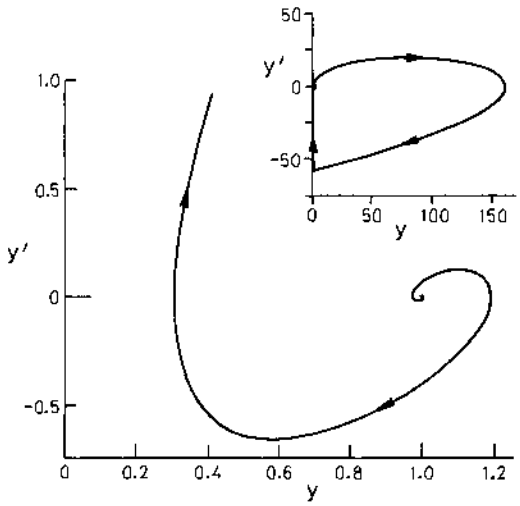

FIG. 3. *Phase-plane (y' versus y) plot for the solution of Fig. 2; the inset is a continuation to large y, y'.*

An alternative way to present the present results is in the form of a phase-plane plot such as that of Fig. 3 (also for $a = .004$), plotting y' versus y. In that plane, (2.2) describes a spiral. All solutions spiral out from $(1, 0)$, continuing to spiral in bigger and bigger loops in $y > 0$, but approaching closer to $y = 0$ with each loop. The insert shows the behaviour of this spiral for larger y, y' values, indicating a maximum upslope of $y' = 19.33$, the super maximum at $y = 160.81$, and an apparently straight-line approach toward the super minimum, the maximum downslope $y' = -58.10$ not being achieved until $y \approx 10^{-10}$.

The conclusion that can be drawn from this work is that there is no solution to the present equation of the type indicated in Fig. 1, i.e., no solution applicable to draining over a dry wall of a layer of semi-infinite extent, since the layer thickness can never be brought to zero at any finite x. The fact that the "primary" minimum thickness can be made very small indeed at some values of a is of interest, as is the fact that the problem has no unique solution, the parameter a being undetermined at this stage.

The choice of the constant "a" as the parameter describing this family of solutions

is in fact rather artificial. For example, having solved for the complete family, we could equally replace a by some output measure of the solution, as the single parameter identifying individual members of that family. Figure 4 shows (solid curve) plots of the primary maximum and primary minimum magnitudes as functions of such a new parameter, namely, the size β of the maximum downslope, that occurs at the inflection point lying between these two turning points. This parameter β plays a role like a contact angle, even though there is no contact, a feature that we shall explore further.

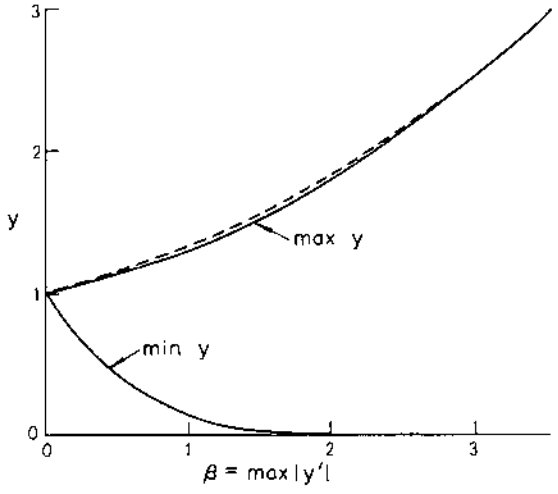

FIG. 4. *Computed primary maxima and minima, as functions of the downslope* $\beta = \max|y'(x)|$ *at the inflection point lying between them. The solid curves are computed by allowing the parameter* a *to vary in the family of dry-wall draining solutions. The dashed maximum is computed by allowing* δ *to vary in the wet-wall draining solution; see Fig. 8 (later) for the relationship between* β *and* δ.

3. Wet wall draining. We now generalise (2.1) to

$$\frac{d^3y}{dx^3} = -1 + \frac{1+\delta+\delta^2}{y^2} - \frac{\delta+\delta^2}{y^3} \tag{3.1}$$

where δ is an input parameter, noting that (3.1) reduces to (2.1) when $\delta = 0$.

Equation (3.1) can be used to describe draining over a wet wall, i.e., a case in which the draining layer is doubly infinite, extending forever down the wall as well as forever up it. Equation (3.1) possesses the two uniform solutions $y \equiv 1$ and $y \equiv \delta$, and we may consider δ as the thickness of a precursor wetting layer. Hence it is appropriate to solve (3.1) subject to the two boundary conditions

$$y \to 1 \quad \text{as} \quad x \to -\infty \tag{3.2}$$

and

$$y \to \delta \quad \text{as} \quad x \to +\infty. \tag{3.3}$$

In fact, even though (3.1) is a third-order ordinary differential equation, the above is a complete specification of a boundary value problem since the absence of x from (3.1) implies again that the origin of x can be specified arbitrarily, eliminating the need for a third boundary condition.

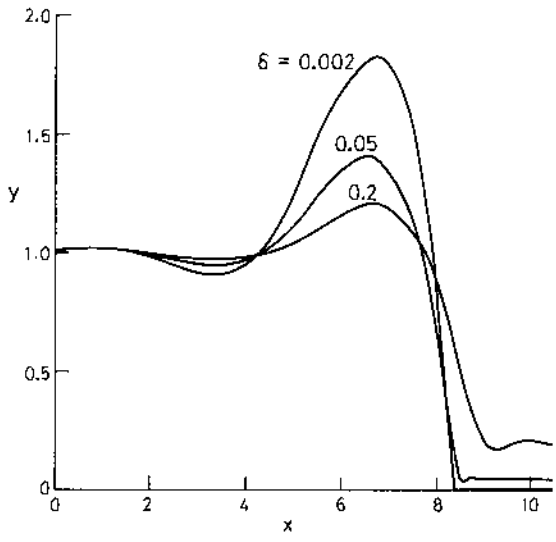

FIG. 5. *Computed solutions $y = y(x)$ for various nonzero δ.*

It appears that the above problem possesses a unique solution for any $\delta \leq 1$, and the results are given in Fig. 5 for various δ values. These results were obtained by numerical means similar to that described in the previous section. That is, we first strengthen (3.2) to

$$y \to 1 + ae^{qx}\cos(q\sqrt{3}x) \tag{3.4}$$

where $q = (2 - \delta - \delta^2)^{1/3}/2$ (and in practice even further by including $O(a^2)$ terms), and then solve the initial-value problem (3.1), (3.4) for various choices of a, choosing a by trial and error until (3.3) is satisfied.

In practice, this trial and error procedure is a search for maxima and minima near $y = \delta$. That is, if a is moderately close to its correct value, we may find that, after oscillating around $y = 1$ and reaching a primary maximum somewhat above $y = 1$, then y plunges apparently toward zero, but at the last moment reaches a (primary) minimum somewhat below $y = \delta$, then increases above $y = \delta$. If we then change a slightly and recompute, we may be able to induce a subsequent maximum just above $y = \delta$, after which y decreases toward zero. So we modify a again slightly and may be able to induce a further (secondary) minimum, even closer to (but just below) $y = \delta$, etc. It is never possible to stop the solution eventually diverging if we keep increasing x toward $+\infty$ (or decreasing x toward $-\infty$), since the exponentially growing solution that has been suppressed in approximations like (3.4) eventually takes over in the form of a numerical instability. But before this happens, the correct value of a can be determined to at least seven significant figures by the above process of creating turning points, and details of the profile such as the size of the primary and secondary maxima and minima are established to at least four significant figures. As in the previous section, the truncation error must then be checked by repeating the computations with a reduced by the factor 37.6224, and in this way consistent four-figure accuracy was verified.

Again the use of (y, y') phase-plane plots clarifies this picture. Now there are

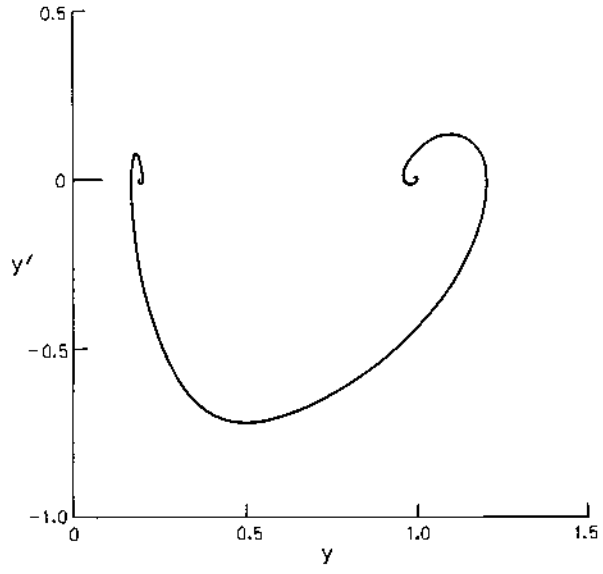

FIG. 6. *Phase-plane plot for the example* $\delta = 0.2$ *of Fig.* 5.

spirals centered on both points $(1,0)$ and $(\delta,0)$, and our numerical task is to connect these two spirals. The result for $\delta = 0.2$ is shown in Fig. 6.

The dashed curve of Fig. 4 shows the primary maximum thickness as a function of the maximum downslope β (which itself varies with δ in a manner to be discussed below) for these solutions. Clearly the present results are in remarkably close agreement with those of §2, for all values of β. If the relationship between β and δ is known, it is clear that a possible method for making the solution of (2.1) unique is to terminate the solution of that equation at an inflection point where the downslope is β, and to choose a value of β that corresponds to the desired δ.

4. Small-δ limit. The limit $\delta \to 0$ is of considerable interest, and this limit is singular, not least because the problem with $\delta = 0$ has no solution for large x. We can treat this limit by matched asymptotic expansions, as follows.

The formal result of setting $\delta = 0$ as in §2 is now viewed as an outer approximation which is valid for $y = O(1)$, but loses its validity near a primary minimum $y = y_0$ at $x = x_0$. The outer approximation is assumed to have been computed at a value of the parameter a such that this primary minimum takes small values y_0, comparable in magnitude to δ.

Now let us seek an inner expansion valid when $x \approx x_0$ and $y = O(\delta)$. Set

$$y = \frac{Y}{\delta}, \quad x = x_0 + \frac{X}{\delta}. \tag{4.1}$$

Then the formal limit of (3.1) as $\delta \to 0$ at fixed X, Y is the differential equation

$$Y''' = Y^{-2} - Y^{-3}. \tag{4.2}$$

Physically, all we have done is to neglect gravity, and rescale, so this is the same ("Landau–Levich") equation as describes various flows involving a force balance between surface tension and viscosity, in the absence of (or with neglect of) gravity.

In the present context, equation (4.2) describes the flow in the neighbourhood of the spiral at $(y, y') = (\delta, 0)$ or $(Y, Y') = (1, 0)$ of Fig. 6, and hence we must solve it subject to the boundary condition

$$Y \to 1 \quad \text{as} \quad X \to +\infty. \tag{4.3}$$

Again, there is a one-parameter family of solutions of (4.2) subject to (4.3), and all members can be found to at least four-figure accuracy by numerical methods directly equivalent to those already discussed, noting that the oscillatory behaviour equivalent to (2.3) now occurs as $X \to +\infty$. However, it turns out that only one member of that family is of present interest, namely, that unique member which has vanishing curvature in the limit as $X \to -\infty$, specifically satisfying

$$Y \to -X\,(3\log|X|)^{1/3} + O(X\log^{-5/3}|X|) \tag{4.4}$$

as $X \to -\infty$.

The most straightforward computational procedure for identifying this special solution is to examine the product $YY'Y''$, which should approach -1 as $X \to -\infty$ when (4.4) holds, whereas it becomes either positively or negatively unbounded like $[Y''(-\infty)X]^3/2$ whenever $Y''(-\infty) \neq 0$. The sign (and ultimately the magnitude) of $YY'Y''$ therefore provides a sensitive test of how close we are to the solution satisfying $Y''(-\infty) = 0$.

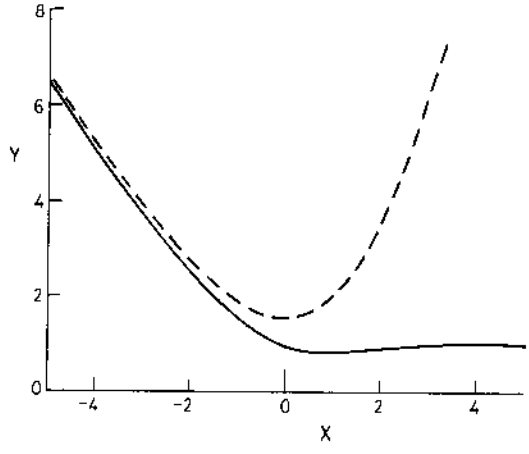

FIG. 7. *Inner (Landau–Levich, solid curve) and intermediate (dashed curve) solutions* $Y = Y(X)$.

Figure 7 (solid curve) shows this unique inner solution. The absolute minimum value of Y is 0.8215 (in reasonable agreement with Tanner's (1979) value of "about" 0.825 and with a solution graph of Friz (1965)), and the subsequent maximum positive value of the slope Y' is 0.1100. These are significant numbers for the general problem, showing that the actual thickness y will always fall to 82 percent of the precursor thickness δ, before recovering and approaching $y = \delta$ in an oscillatory manner, with a maximum slope of 0.11. These results are confirmed by the numerical solutions of §3 at small finite δ.

In order to match these inner and outer approximations, we must consider the inner limit of the outer problem and the outer limit of the inner problem. It is of

interest to observe first that if y is small in (2.1) or if Y is large in (4.1), we arrive at the same "intermediate" differential equation

$$z''' = z^{-2} \tag{4.5}$$

with z for either y or Y.

Equation (4.5) is yet another differential equation that is of interest in its own right; see Tanner (1979). However, unlike the others so far considered, there is no uniform solution, and the phase plane topology is not a spiral. The solutions of interest to us have a single minimum $z = z_0$, which can be located at $x = 0$ without loss of generality. If we scale

$$z = z_0 Z(X) \quad \text{with} \quad X = \frac{x}{z_0} \tag{4.6}$$

then $Z(X)$ satisfies the same equation (4.5), namely,

$$Z''' = Z^{-2} \tag{4.7}$$

and is to be solved subject to the initial conditions

$$Z(0) = 1, \qquad Z'(0) = 0. \tag{4.8}$$

Thus, again we have a one-parameter family of solutions, the parameter being the value of the initial curvature $Z''(0)$, and all members of this family can be found numerically without difficulty.

Within this family there is a unique member parametrised by $Z''(0) = 1.2836$, having zero curvature at $X = -\infty$ and hence satisfying (4.4); this member has finite nonzero curvature $Z''(+\infty) = 2.1591$ at the other extreme $X \to +\infty$, and is shown (scaled, see below) as the dashed curve of Fig. 7.

Let us now make use of this fully determined intermediate solution $Z(X)$ as the link between the inner and outer approximations, as follows. First we assume that the inner approximation $Y(X)$ merges smoothly with the intermediate approximation (shifted and scaled suitably) for large negative X, writing in that regime

$$Y(X) \to z_0 Z\left(\frac{X - X_0}{z_0}\right) \tag{4.9}$$

for some z_0 and X_0 to be determined.

Note that since both Y and Z satisfy the boundary condition (4.4) as $X \to -\infty$ already, (4.9) says quite a bit more than (4.4). Indeed, (4.4) can be seen to be the leading term in a series of negative powers of $\log^2 |X|$, every term of which is uniquely determined by the leading term, and hence is common to both Y and Z irrespective of the value of z_0. In practice, we must compute both Y and Z to high accuracy for a range of large negative X, and then choose both z_0 and X_0 so that (4.9) holds as accurately as possible over that range. This is a difficult numerical task, and our final result $z_0 = 1.54$ has only about 1 percent accuracy. The value X_0 of the shift in the intermediate minimum is of no significance, since the origin of X in the inner solution is in any case arbitrary. But once it is fixed, the result is the dashed curve of Fig. 7, showing clearly the smooth merger between inner and intermediate solutions as $X \to -\infty$.

Now let us consider the intermediate limit of the outer approximation. That is, let us assume that when the actual thickness y is small compared to unity, the outer solution also approaches a shifted and scaled multiple of the intermediate solution, namely,

$$y(x) \to y_0 Z\left(\frac{x - x_0}{y_0}\right). \tag{4.10}$$

But in this case, the minimum at (x_0, y_0) is known in advance.

Finally, we match by demanding that (4.9) and (4.10) are identical, and, using the definition (4.1) of Y (and ignoring the arbitrary X-shift X_0), this is true if

$$y_0 = z_0\delta \approx 1.54\delta. \tag{4.11}$$

This is again a result of some significance, providing the link between outer computations done as in §2 with $\delta = 0$, and the actual small but nonzero value δ of the precursor thickness. That is, if δ is given, we simply choose that member of the one-parameter family of outer solutions which has a primary minimum thickness 54 percent higher than the precursor thickness. This principle is confirmed by the computations of §3, i.e., with this choice, there is close agreement between solutions of (2.1) and (3.1) at all values of x.

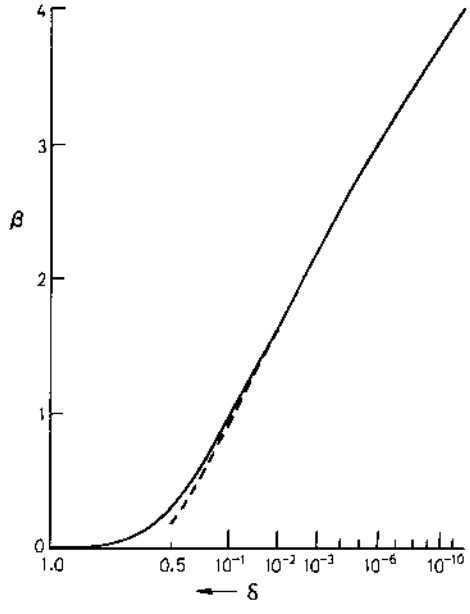

FIG. 8. *Maximum slope* $\beta = \max|y'(x)|$ *as a function of* δ; *note the logarithmic scale, with* δ *becoming (extremely) small toward the right of the figure. The solid curve is the direct computation for general nonzero* δ. *The dashed curve is the asymptotic theory for small* δ.

For example, Fig. 8 shows a plot of the maximum downslope $\beta = \max|y'|$ as a function of δ, on a logarithmic scale such that the abscissa is actually $(-\log\delta)^{1/3}$. The solid curve is that from computations based on the finite-δ theory of §3, whereas the dashed curve is based on assuming that $\delta = 0$ in the differential equation as in §2, but with a primary minimum selected proportional to δ according to (4.11). The small-δ asymptotic results are within 1 percent of the finite-δ computations for $\delta < 0.05$.

In fact, Fig. 8 is of special importance for the outer problem. The maximum downslope $y' = -\beta$ occurs well into the outer region, at a point that only very slowly approaches zero thickness as $\delta \to 0$; for example, it still occurs at about $y = 0.1$ when

$\delta = 10^{-7}$. Not only that, but the maximum in the downslope is very broad for small δ. For example, when $\delta = 10^{-7}$, it is not until about $y = 0.0015$ that the downslope has fallen to 90 percent of its peak value, and not until about $y = 10^{-6}$ has it reached half of its peak value. To all intents and purposes, the thickness appears to be approaching zero linearly (as in the insert to Fig. 3), with a downslope insignificantly different from β, until y is too small to be detected by an outer observer.

This behaviour is as if zero thickness were possible even when $\delta = 0$, with a prescribed contact angle whose tangent is β. Hence if, as is the case in numerical studies of problems more complicated than the present one, it is impractical to perform computations on length scales comparable to δ, we may ignore the precursor layer altogether. However, when doing so, we must make the problem unique by specifying an apparent contact angle, of a magnitude whose value can be related to the precursor thickness δ via Fig. 8. To the extent that this curve is close to a straight line, this implies that the apparent contact slope can be considered as proportional to the one-third power of the logarithm of the precursor thickness, an idea first suggested by Tanner (1979); see also de Gennes (1985); however, the actual relationship between β and δ is as computed in the present study and plotted in Fig. 8.

5. Model equations that allow slip. The equations

$$\frac{d^3y}{dx^3} = -1 + \frac{1+\alpha}{y^2+\alpha} \tag{5.1}$$

and

$$\frac{d^3y}{dx^3} = -1 + \frac{1+\alpha}{y^2+\alpha y} \tag{5.2}$$

are generalisations of (2.1), reducing to that equation when $\alpha = 0$, with the property that, for $\alpha \neq 0$, each serves to mitigate the singularity at $y = 0$ that prevents contact between the liquid surface and the solid wall. They each relax the no-slip condition on the wall, and are based on the assumption that, for some slip coefficient $A = A(y)$,

$$u = Au_z \tag{5.3}$$

at $z = 0$. Here u is the fluid velocity parallel to the wall and z is the space coordinate perpendicular to the wall. They have their origin in a conjecture due originally to Navier (see, e.g., Panton (1984, pp. 149ff)) that the velocity of slip at the wall should be proportional to the shear stress there. Although such slip (if present at all) is almost always negligible, contact without slip involves an infinite surface traction in the present context. Since this is replaced by a finite surface traction when slip with any nonzero value of A is allowed, a slip law of this form represents a plausible alternative to requiring a wetting layer.

In the first model, due to Greenspan (1978), the slip coefficient is taken to be

$$A = \alpha/(3y) \tag{5.4}$$

where α is constant. For the present problem, this choice leads to the differential equation given in (5.1), where $\alpha^{1/2}$ and y are measured in multiples of the actual layer thickness far from the front. The contact point where $y = 0$ is no longer singular, and the slope and higher derivatives may be finite there. The dependence on y in (5.4)

is chosen so that the effect of the slip is greatest when $y << 1$, i.e., near the contact point.

The alternative (5.2) follows from a slip model of Hocking (1981), in which

$$A = \alpha \tag{5.5}$$

where α is again a (different) constant. Near $y = 0$, the most singular part of the solution is given by

$$y = \left[\frac{8}{3\alpha}\right]^{1/2} (x_0 - x)^{3/2} \tag{5.6}$$

which satisfies the equation (5.2) in the limit $y << \alpha$. Both models (5.1) or (5.2) can be criticised for allowing some unphysical measure of slip throughout the flow, not just at $y = 0$, (5.2) more than (5.1).

Numerically, either equation can be solved as an initial-value problem, by a method similar to that described in §3. The starting solution is

$$y = 1 + ae^{qx}\cos(q\sqrt{3}x) \tag{5.7}$$

where q is either $2^{-2/3}(1+\alpha)^{-1/3}$ for (5.1), or $2^{-1}(2+\alpha)^{1/3}(1+\alpha)^{-1/3}$ for (5.2), and the origin of x is arbitrary. The parameter a is free, and, as previously explained, must be taken to be a small number. For every given choice of α, the entire family of solutions that asymptote to $y = 1$ as $x \to -\infty$ is generated by allowing a to vary within a range defined by the factor 37.6224. Thus there is really a two-parameter family of solutions, the initial parameters being α and a. As x increases, the function

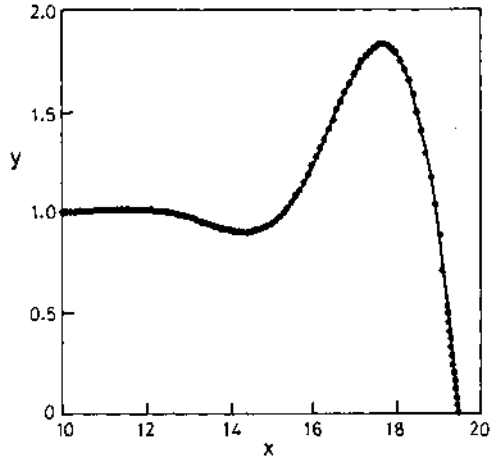

FIG. 9. *Comparison of wetting-layer and slip models. The wetting-layer result (solid line) uses* $\delta = 0.002$. *The slip result (symbols) is the solution of* (5.2) *with* $\alpha = 0.0001$. *The free parameter in the slip model has been adjusted so that the maximum* y *values are the same.*

$y(x)$ oscillates within a growing envelope until the curve meets the axis $y = 0$.

For a range of values of α, it is possible to closely approximate a given profile generated by the wet-wall model of §3. Figure 9 shows a comparison between the wetting-layer result for $\delta = 0.002$, as in Fig. 5, and a calculation from (5.1) using

$\alpha = 0.0001$ and a value of the parameter a that was chosen so that the maximum overshoot was the same. The curves are almost indistinguishable; for example, the value of the maximum downslope agrees to three decimal places. The downslope at the actual contact point, which may be thought of as an independent parameter in the slip model replacing the nonphysical parameter a, is equal to 0.689. The rather large change in downslope from this value to the maximum downslope of 2.01 at the inflection point occurs for $y < 0.01$, and is not discernible on the scale of the figure. An essentially equivalent result has also been obtained using the alternative model (5.2) with $\alpha = 0{,}01$. In that case the contact slope magnitude is 0.30.

The range of the slip parameter α that is needed to approximate a given profile is by no means arbitrary. The choices of α used here are close to the *minimum* permissible values; slightly smaller values will yield solution families whose minimum overshoot is greater than the value 1.822 in Fig. 9. For a given value of α, the minimum overshoot corresponds to a profile that meets the wall at zero slope. Any further reduction in α is unacceptable, since it will yield a positive minimum value of y and a subsequent very large overshoot on the next cycle. On the other hand, large values of α are not acceptable either. Values of α greater than about 0.1 result in significant changes in the basic undulation wavelength at $O(1)$ values of y, reflecting influences in regions far from contact, where the slip assumption is untenable.

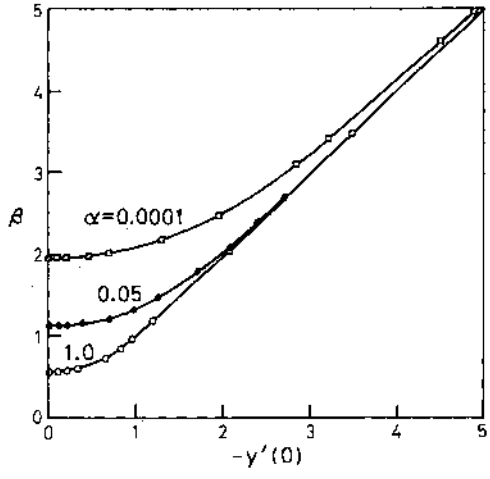

FIG. 10. *Maximum downslope versus downslope at the wall, for three values of the slip parameter α in* (5.2).

The lower bound on α is illustrated more clearly in Fig. 10, where the magnitude of the maximum slope $\beta = \max |y'|$ is plotted versus the contact slope (i.e., the value of $-y'$ at $y = 0$) for several values of the parameter α. These results used the model (5.1), but a similar family of curves can be obtained for the model (5.2). For small contact slope, the maximum slope reaches a limiting value whose magnitude increases as the slip parameter α is reduced. For any value of α, the maximum slope becomes close to the contact slope when they are both large. For the model (5.2) this approach is asymptotic, since the inflection point occurs for $y > 0$ and only approaches $y = 0$ in the limit $\alpha \to 0$. For the model (5.1), on the other hand, the inflection point may move through $y = 0$; thus there is a finite range of values of α where the two slopes are equal.

It is interesting to inquire to what extent the slope at contact and the maximum slope may be identified with the static and dynamic contact angles, respectively. The static contact angle is a rather well-understood, reproducible, and tabulated quantity for drops of liquid on a clean surface. The so-called dynamic contact angle is somewhat more controversial and is, in addition, is often considered to be an "apparent" quantity because of the ill-defined nature of the conditions in the near vicinity of the contact point. The advancing contact angle, for motion onto a previously dry surface as we consider here, is known to be an increasing function of contact line speed. (See Dussan (1979) for an extensive discussion.)

With $\tan\theta_s$ (="slope at contact") and $\tan\theta_d$ (="maximum slope") corresponding to the quantities plotted in Fig. 10, we must return temporarily to dimensional variables, now written uppercase. For the coating flow problem considered here, the appropriate scaling is

$$\begin{aligned} Y &= Y_\infty y, \\ X &= Y_\infty (3\mathrm{Ca})^{-1/3} x, \end{aligned} \tag{5.8}$$

where $\mathrm{Ca} = \mu U/\sigma$ is a capillary number and U, μ and σ are contact line speed, fluid viscosity, and surface tension, respectively. Thus the angles Θ in the physical problem are related to those used here ($\tan\theta = y'$) by

$$\tan\Theta = (3\mathrm{Ca})^{1/3} \tan\theta. \tag{5.9}$$

If we consider the static contact angle Θ_s to be a given material constant for a given physical system, then for motion at some speed U and hence some definite value of Ca, the corresponding value of $\tan\theta_s$ computed from (5.9) can be located on the horizontal axis in Fig. 10. Depending on the chosen value of the slip coefficient α, the value of θ_d is then determined by reading off the vertical axis of this graph. Finally, the actual dynamic contact angle Θ_d is determined by reverting to (5.9). The resulting functional dependence $\Theta_d = \Theta_d(\Theta_s, \mathrm{Ca})$ exhibits the important qualitative features of the dependence of contact angle on speed U shown by Dussan (1979).

For simplicity, any of the curves in the figure can be acceptably fitted by the formula

$$\tan\theta_d = \left[\tan^3\theta_{\min}(\alpha) + \tan^3\theta_s\right]^{1/3} \tag{5.10}$$

or, in physical variables, by

$$\tan\Theta_d = \left[3\mathrm{Ca}\ \tan^3\theta_{\min}(\alpha) + \tan^3\Theta_s\right]^{1/3} \tag{5.11}$$

where $\tan\theta_{\min}$ is the value of the maximum downslope when the contact angle is zero (i.e., the value of the intercept on the vertical axis of Fig. 10) and is thus a computable function of α. For very small speeds, the difference $\tan\Theta_d - \tan\Theta_s$ is a linear function of Ca and hence of U, while at relatively high speeds, "Tanner's law" (Tanner (1979)), $\tan\Theta_d = \mathrm{const.}U^{1/3}$ is recovered.

REFERENCES

[1] R. W. Atherton and G. M. Homsy, *On the derivation of evolution equations for interfacial waves*, Chem. Engrg. Comm., 2 (1976), p. 57.

[2] F. P. Bretherton, *The motion of long bubbles in tubes*, J. Fluid Mech., 10 (1961), pp. 166–188.
[3] B. Cox, *The dynamics of the spreading of liquids on a solid surface. Part 1: Viscous flow*, J. Fluid Mech., 168 (1986), pp. 169–194.
[4] E. B. Dussan V, *On the spreading of liquids on solid surfaces: static and dynamic contact angles*, Ann. Rev. Fluid Mech., 11 (1979), pp. 371–400.
[5] ———, *The moving contact line: the slip boundary condition*, J. Fluid Mech., 77 (1976), pp. 665–684.
[6] A. Friedmann, *Unsolved mathematical issues in coating flow mechanics*, *Mathematics in Industrial Problems*, Chap. 3, Springer-Verlag, Berlin, New York, 1988.
[7] G. Friz, *Über der dynamischen Randwinkel im Fall der vollständigen Benetzung*, Z. Angew. Phys., 19 (1965), pp. 374–378.
[8] P. G. de Gennes, *Wetting: statics and dynamics*, Rev. Modern Physics, 57 (1985), pp. 827–863.
[9] H. Greenspan, *On the motion of a small viscous droplet that wets a surface*, J. Fluid Mech., 84 (1978), pp. 125–143.
[10] H. Greenspan and B. M. McCay, *On the wetting of a surface by a very viscous liquid*, Stud. Appl. Math., 64 (1981), pp. 95–112.
[11] L. M. Hocking, *Sliding and spreading of thin two-dimensional drops*, Quart. J. Mech. Appl. Math., 34 (1981), pp. 37–55.
[12] F. A. Howes, *The asymptotic solution of a class of third-order boundary-value problems arising in the theory of thin film flows*, SIAM J. Appl. Math., 43 (1983), pp. 993–1004.
[13] C. Huh and L. E. Scriven, *Hydrodynamic model of steady movement of a solid/liquid/fluid contact line*, J. Colloid Interf. Sci., 35 (1971), pp. 85–101.
[14] H. E. Huppert, *Flow and instability of a viscous current down a slope*, Nature, 300 (1982), pp. 427–429.
[15] L. Landau and V. G. Levich, *Dragging of a liquid by a moving plate*, Acta Physicochim. U.R.S.S., 17 (1942), pp. 42–54.
[16] V. G. Levich, *Physicochemical Hydrodynamics*, Prentice–Hall, Englewood Cliffs, NJ, 1962.
[17] R. L. Panton, *Incompressible Flow*, Wiley, New York, 1984.
[18] K. J. Ruschak, *Coating flows*, Ann. Rev. Fluid Mech., 17 (1985), pp. 65–89.
[19] L. W. Schwartz, *Viscous flows down an inclined plane: instability and finger formation*, Phys. Fluids (A), 1 (1989), pp. 443–445.
[20] L. W. Schwartz, H. M. Princen, and A. D. Kiss, *On the motion of bubbles in capillary tubes*, J. Fluid Mech., 172 (1986), pp. 259-275.
[21] L. W. Schwartz and E. E. Michaelides, *Gravity flow of a viscous fluid down a slope with injection*, Phys. Fluids, 31 (1988), pp. 2739–2741.
[22] R. P. Spiers, C. V. Subbaraman, and W. L. Wilkinson, *Free coating of a Newtonian liquid onto a vertical surface*, Chem. Engrg. Sci., 29 (1974), pp. 389–396.
[23] L. Tanner, *The spreading of silicone oil drops on horizontal surfaces*, J. Phys. (D), 12 (1979), pp. 1473–1484.
[24] E. O. Tuck, M. Bentwich, and J. Van der Hoek, *The free-boundary problem for gravity-driven unidirectional viscous flows*, IMA J. Appl. Math., 30 (1983), pp. 191–208.
[25] E. O. Tuck and J.-M. Vanden-Broeck, *Influence of surface tension on jet-stripped continuous coating of sheet materials*, Amer. Inst. Chem. Engrg. J., 30 (1984), pp. 808–811.
[26] S. D. R. Wilson, *The drag-out problem in film coating theory*, J. Engrg. Math., 16 (1982), pp. 209–221.
[27] G. W. Young and S. H. Davis, *On asymptotic solutions of boundary-value problems defined on thin domains*, Quart. Appl. Math., 42 (1985), pp. 403–409.
[28] ———, *Rivulet instabilities*, J. Fluid Mech., 176 (1987), pp. 1–31.